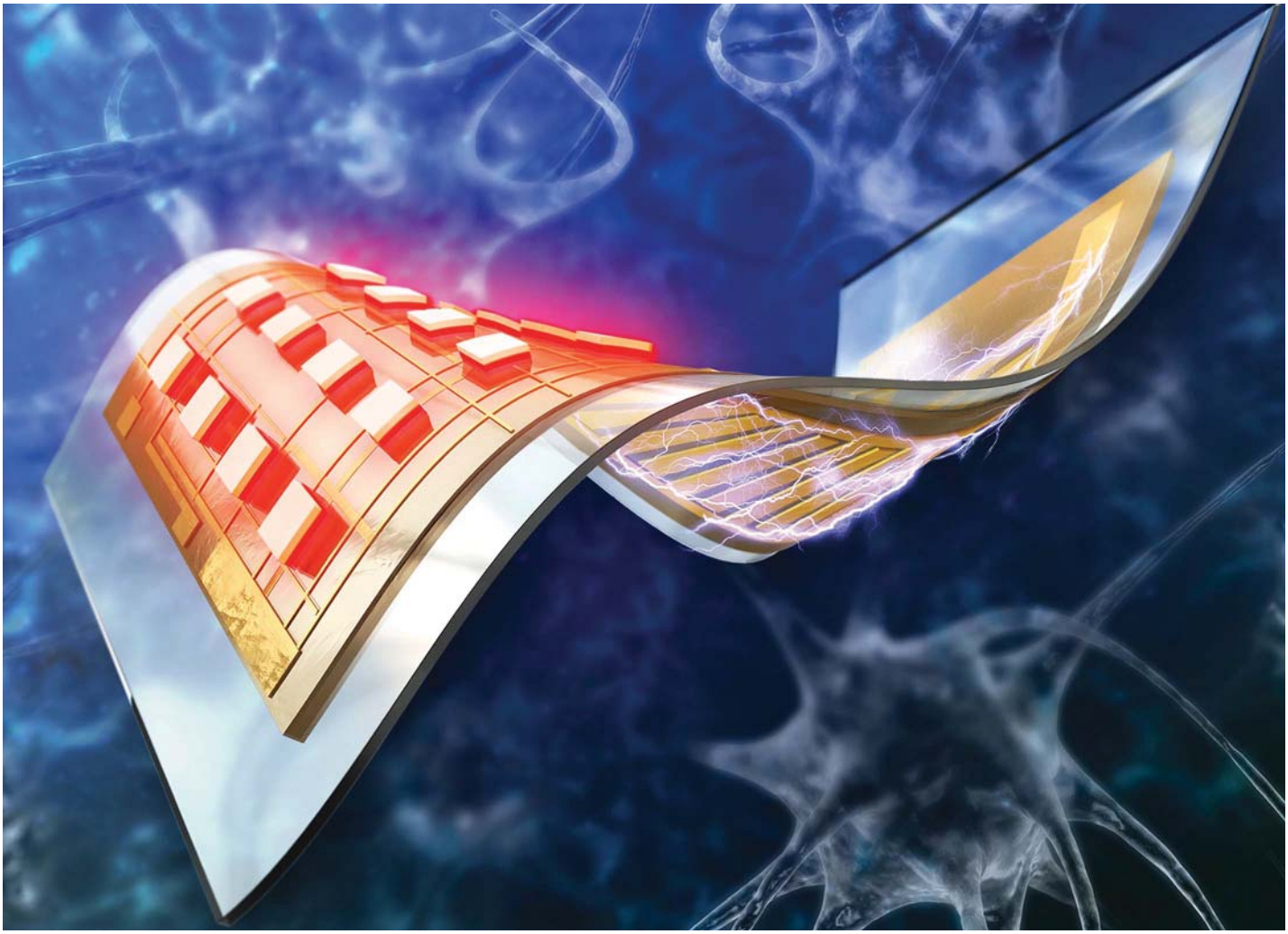

Showcasing research from Prof. Keon Jae Lee's group at Korea Advanced Institute of Science and Technology (KAIST), Republic of Korea.

Title: Self-powered fully-flexible light-emitting system by flexible energy harvester

A self-powered fully-flexible light-emitting system is achieved by a high-performance and flexible piezoelectric thin film energy harvester connected with highly-stable flexible vertical-structured light-emitting diodes (f-VLEDs). The reliable f-VLEDs can be fabricated by using an anisotropic conductive film and sufficiently operated by the generated electricity from the flexible energy harvester.

As featured in:

See Keon Jae Lee *et al.*, *Energy Environ. Sci.*, 2014, **7**, 4035.

ROYAL SOCIETY OF CHEMISTRY

www.rsc.org/ees

Registered charity number: 207890

Energy & Environmental Science

PAPER

View Article Online
View Journal | View Issue

Cite this: *Energy Environ. Sci.*, 2014, **7**, 4035

Self-powered fully-flexible light-emitting system enabled by flexible energy harvester†

Chang Kyu Jeong,‡ Kwi-Il Park,‡ Jung Hwan Son,‡ Geon-Tae Hwang, Seung Hyun Lee, Dae Yong Park, Han Eol Lee, Hwan Keon Lee, Myunghwan Byun and Keon Jae Lee*

Received 1st August 2014
Accepted 14th August 2014

DOI: 10.1039/c4ee02435d

www.rsc.org/ees

Energy-harvesting technology utilising mechanical energy sources is a promising approach for the sustainable, independent, and permanent operation of a variety of flexible electronics. A new concept of a fully-flexible light-emitting system, self-powered by a high-performance piezoelectric thin-film energy harvester has been first established by manipulating highly-robust, flexible, vertically structured light emitting diodes (f-VLEDs). The f-VLEDs fabricated by anisotropic conductive film bonding and entire wafer etching show stable and durable performances during periodic mechanical deformations. A high-output energy harvester capable of generating up to 140 V and 10 μA can be fabricated *via* laser lift-off (LLO) process widely used in industries, in a safe and robust manner. In particular, this LLO process is of great benefit for the fabrication of mechanically stable, flexible piezoelectric devices, without causing any degradation of piezoelectric properties. In this process, self-powered all-flexible electronic system with light emittance can be spontaneously achieved by the electricity produced from flexible thin-film generator by applying slight biomechanical energy without any externally applied energy storage. This conceptual technology of self-powering based on the conversion of mechanical energy to electrical energy can open a facile and robust avenue for diverse, self-powered, bio-implantable applications, as well as commercial display applications.

Broader context

Sustainable and renewable energy-conversion technologies with alternative resources (*e.g.*, solar, wind, thermal, *etc.*) have been under significant development ever since environmental pollution and global warming by fossil fuels were considered to be grave problems. However, most of the outdoor energy sources are unsuitable for an isolated environment, such as the insides of social infrastructures and organism bodies. Because piezoelectric energy-harvesting systems can directly convert mechanical energy into electricity, the piezoelectric energy harvesters have been considered to be a promising power source for wearable optoelectronic devices and bio-implantable applications. Recently, there have been various elegant studies for energy-harvesting technology. However, the concept of a self-powered all-flexible electronic system is unprecedented due to technological limitations of fabricating high-performance flexible energy harvesters for device operation. Recently, the excellent performances of flexible thin film-based energy harvesters have been developed by using the simple and commercialised fabrication, 'laser lift-off (LLO)'. The present work has introduced the self-powered all-flexible light-emitting system based on the novel energy-harvesting technology, and the reliably operated flexible, vertically structured, inorganic, light-emitting diode array fabricated by a commercial anisotropic conductive film bonding approach, thus envisioning a new platform to realise the self-powered fully-flexible electronics with widely accessible biomechanical energy.

Introduction

For the last six years, we have been studying flexible energy harvesting technology[1–7] and inorganic-based flexible electronics[8–14] with the purpose to achieve 'self-powered flexible electronic systems' which can control over the energy source for the operation of high-performance flexible electronic devices in a sustainable, prolonged, remote, and independent manner without the integration of external energy sources. The flexible self-powered systems can be potentially applied for wearable electronics, artificial skin devices, and even to bio-implantable/human-integrated applications.[15,16] In particular, the bio-

Department of Materials Science and Engineering, Korea Advanced Institute of Science and Technology (KAIST), 291 Daehak-ro, Yuseong-gu, Daejeon 305-701, Republic of Korea. E-mail: keonlee@kaist.ac.kr

† Electronic supplementary information (ESI) available: Fig. S1–S16 (detailed methods, detailed structure of epitaxy, magnified current signals, XRD data, Raman spectra, PFM & AFM analyses, SEM images, optical micrographs, FEA simulation, generated signals by a wrist, *etc.*), calculation for the laser penetration depth and heat diffusion length of the PZT, calculation for the mechanical neutral plane and the effective strain in PZT thin film, calculation for the energy conversion efficiency, and ESI Video S1. See DOI: 10.1039/c4ee02435d

‡ These authors contributed equally to this work.

implantable, self-powered flexible systems may have considerable impacts as 'all-flexible electronic systems' in future bioelectronics.[17,18] Although various types of flexible energy harvesting devices have been developed using photovoltaic effects[19,20] or thermoelectricity,[21–23] all-flexible self-powered electronics have not been achieved because of their complicated structures, weather/temperature/place dependencies and low output power efficiency problems. However, a flexible energy harvester using mechanical energy sources, called as piezoelectric energy harvester, has been significantly considered as a highly independent and reliable alternative energy source due to its broad and easy accessibility in our life and nature,[24,25] such as the movements of machines, public transportation, human activities and even the activities of internal organs (*e.g.*, heart, lung, muscle, and blood vessels).[15,26] The concept of a fully-flexible self-powered electronic system using biomechanical energies has been attempted by many researchers, in particular for biomedical applications that require highly flexible, thin, and lightweight systems that enable conformal contacts on the curvilinear and cramped biological organs/tissues.[27–29] Various biomedical devices should be in totally isolated *in vivo* conditions or on moving biological bodies, which are difficult to provide electrical energy from external power supplies. In addition, recent broad interests in the research fields of flexible electronics such as electronic-skin, implantable/wearable systems, and body sensor network (BSN) inevitably require self-powering flexible energy sources to avoid using traditional bulky-type energy sources or chargers. However, to realise such a self-powered fully-flexible electronic system, there are still many critical issues to be resolved, such as the need for a piezoelectric energy harvester with both mechanical flexibility and high-output performance, along with the challenging development of power-efficient flexible electronics. Recently, we have successfully demonstrated breakthrough technology for a high-performance, lightweight, and flexible thin film energy harvesters with an output voltage of more than ~200 V or current of up to ~220 μA, which can serve as a new alternative energy source for driving not only high-level commercial circuit units but also a biocompatible cardiac pacemaker for directly stimulating animal heartbeats without the timely replacement of batteries.[5,7] This outstanding new energy-harvesting technology, based on a piezoelectric thin film on a very thin flexible plastic substrate is a strong candidate for the power source of self-powered flexible systems because it can scavenge mechanical energy even from diverse biological motions. However, previously studied piezoelectric energy-harvesting technologies are shadowed by the limited applications of flexible electronics caused by the lack of mechanical flexibility and low performance, as well as the incompatibility between the piezoelectric generators and flexible electronics. With these necessities and capabilities, energy-efficient flexible electronics combined with flexible energy harvesters, which has never been studied due to their incompatibility, should be developed to build self-powered human-integrated electronics.

Flexible III–V inorganic light-emitting diodes (LEDs), which enable conformal and intimate contacts to the curvilinear surface have attracted increasing attention from numerous researchers in the fields of biomedical applications, as well as that of flexible displays.[30–33] The flexible inorganic LEDs have been largely studied because of their excellent robustness, long life-span, and light emission for *in vivo* biomedical applications (*e.g.*, optogenetic stimulators and phototherapy).[34–37] However, most of the previously demonstrated flexible inorganic LEDs were reported as laterally structured LEDs that possibly caused low efficacy or fatal organ damage, resulting from inevitable drawbacks such as poor current spreading, significant heat generation, and narrow light-emitting areas.[38,39] Despite the recently developed flexible vertical LED by using transfer stamping and cold welding,[40] challenges still exist for overcoming drawbacks such as the complex fabrication steps and the potential mechanical damage on the physically harsh process, hindering mass commercialisation.

In this work, we demonstrate self-powered all-flexible light-emitting optoelectronics composed of flexible vertically structured AlGaInP-based LEDs and a flexible, high-output piezoelectric energy harvester. Stable, reliable, easily processable red light-emitting, flexible, and vertically structured LEDs (f-VLEDs) were fabricated using anisotropic conductive film (ACF) bonding and simple wet etching of the entire GaA mother wafer. The characteristics of our f-VLEDs are stably maintained on bending with a radius as small as 3 mm and 1000 bending cycles. We also confirmed that the well-designed f-VLEDs are electrically compatible to the alternating current (AC)-pulsed power source of a flexible piezoelectric energy harvester. The flexible $PbZr_{0.52}Ti_{0.48}O_3$ (PZT) thin film-based energy harvester is made by a laser lift-off (LLO) process. Transferring the PZT thin film from a sapphire wafer to a plastic substrate using an XeCl-pulsed excimer laser does not cause the degradation of piezoelectric properties.[5] The final flexible piezoelectric energy harvester generates high-output electricity (up to ~140 V and 10 μA) during bending/releasing stimulation, and the resulting electrical energy converted from subtle fingering motions is sufficient to readily turn on the f-VLEDs array, dispensing with the need for external energy sources.

Results and discussion

Design and fabrication of a self-powered flexible light-emitting system

A self-powered flexible light-emitting system based on thin-film piezoelectric energy harvesters was constructed as schematically illustrated in Fig. 1. Initially, we prepared the red emitting f-VLED from a GaAs wafer with device epitaxial layers at the top (thickness in 7.28 μm), as shown in Fig. 1a, S1 and S2 in ESI.† Vertical LEDs have excellent advantages such as improved light-extraction efficiency, reliable heat sinking, and good current spreading, arising from the intrinsic structure. The peak wavelength of photoluminescence (PL) from our designed epitaxial LED multi-quantum well (MQW, Fig. S2†) was about 645 nm (Fig. S4 in ESI†). The choice of this wavelength was strongly motivated by the fact that red-light emissions can be useful for diverse biomedical applications, such as optogenetic neural stimulation using the channel protein 'Chrimson',[41] as well as phototherapy using thermal or non-thermal treatments.[37,42,43]

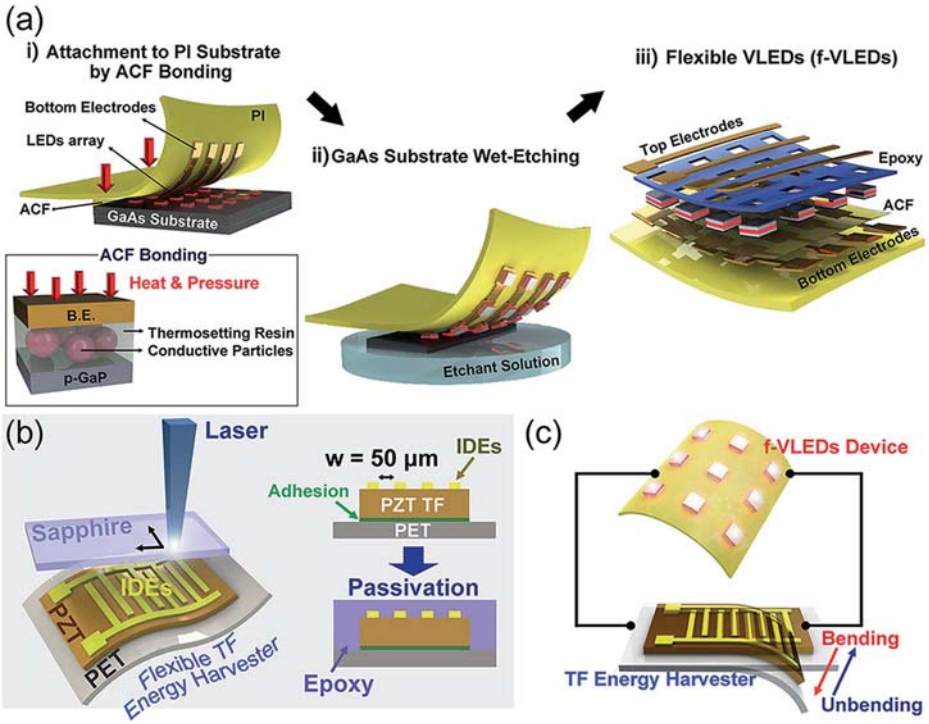

Fig. 1 Schemes for a self-powered flexible light-emitting system. Illustrations showing the fabrication steps of: (a) red emitting f-VLEDs with MQW layers; and (b) a flexible thin-film (TF) energy harvester. (c) Schematics of the final self-powered flexible light-emitting system.

After the dry etching of MQW epitaxial layers to isolate VLED chips, an electrode-patterned polyimide (PI) plastic substrate was firmly attached to the VLED chips using an ACF bonding process (Fig. 1a-i). The ACF composed of metallic micro-particles and polymeric resin becomes conductive by applying mild pressure at an elevated temperature (245 °C). This type of an interconnection method is currently used in the semiconductor industries to form conductive paths in an anisotropic and vertical mode.[44,45] The subsequent step involves removal of the GaAs mother wafer by wet etching using ammonium hydroxide and hydrogen peroxide solutions (Fig. 1a-ii and S3†), followed by epoxy passivation and top-electrode deposition (Fig. 1a-iii). Previously reported flexible inorganic red LEDs were based on the complicated fabrication procedure, which can be summarized as the removal of interfacial sacrificial layers.[30,40,46] These approaches had critical drawbacks such as significant cost increase, the difficulty of growing epitaxial layers on unusual sacrificial layers, and the incompatibility with the current LED industry. Moreover, processing yields and technological accessibility can become considerably low because of the size limitations and complex steps caused by the side-directional/narrow-gap sacrificial-layer etching and transfer-stamping protocols.[47,48] However, our approach in this work used the facile and industrially-friendly technology, 'removal of entire bottom GaAs wafer', to successfully achieve f-VLEDs on plastic substrates without the undercut-etched sacrificial layers. This wet etching of the entire bottom GaAs wafer is widely known in commercialised bulk LEDs technology because of its simple and short fabrication process (~30 min). In addition, the ACF bonding method applied to this work is also widely used in recent packaging processes of the display industry. The ACF plays simultaneous roles of both an adhesion layer to the plastic substrate and a vertical conduction layer to the bottom electrodes. This technology easily formed electrode contacts to the n and p sides of the VLED structures by planar microelectronic fabrication without complex printing transfer or welding techniques. In this work, the rational design of fabrication for the commercialization of f-VLEDs was enabled by all industrially-friendly technologies. We believe that our approaches possibly open a robust platform for flexible inorganic optoelectronics, which provide a platform towards practical applications of all-flexible inorganic optoelectronics.

A flexible PZT thin-film energy harvester as a self-powered flexible energy source for the f-VLEDs was built by the LLO process, which is generally used for blue VLEDs to safely separate GaN film from a sapphire substrate (Fig. 1b). The PZT thin film (2 μm in thickness) was deposited on a sapphire substrate by spin-casting a conventional sol–gel solution. After subsequent pyrolysis and calcination, the crystallised PZT thin film on the sapphire wafer was fixed to a flexible polyethylene terephthalate (PET) substrate by an ultraviolet (UV) light-enabled curing of polyurethane (PU) adhesive. Irradiating the backside of a sapphire substrate with the XeCl-pulsed excimer laser can transfer the PZT thin film to the flexible plastic substrate because the photon energy of XeCl laser (4.03 eV) is smaller than the band-gap energy of sapphire (8.7 eV) and larger than that of PZT (3.2–3.6 eV). Consequently, the laser beam can penetrate the sapphire substrate, followed by the partial

melting and dissociation of the PZT at the interface with the sapphire (see ESI†).[5,49] By employing an optimum laser-beam energy density (420 mJ cm^{-2}), the entire area of the piezoelectric PZT thin film (2 cm × 5 cm) can be transferred stably onto the plastic substrate without degradation of piezoelectric properties (Fig. S7†). It is noteworthy that the energy density of the irradiated laser beam plays a critical role in the separating and transferring of the PZT thin film. At much lower energy density ($\ll$420 mJ cm^{-2}), the PZT thin film was neither detached nor transferred from the sapphire substrate, while at much higher energy density ($\gg$420 mJ cm^{-2}) mechanical damage and physical ablation were caused. Au interdigitated electrodes (IDEs) with finger widths of 100 μm and gaps of 50 μm were formed on the transferred PZT thin film through sputtering and standard microfabrication processes. The critical design parameters for the IDEs include the finger width, inter-electrode gap (spacing), and the number of IDE fingers. The compact IDE fingers (narrow inter-electrode gap) of the PZT thin-film energy harvester were selected to enhance the output current because more IDE fingers can produce higher currents from the IDE-type energy harvester compared to less dense IDE fingers.[5] Whereas sandwich-type electrodes (*i.e.*, metal–insulator–metal, MIM) have a lack of control over piezoelectric layer thickness for enhancing output; the spacing between the adjacent electrode fingers of IDEs can be readily tuned to achieve a high-performance flexible energy harvester. Although the narrow IDE gaps result in a partial reduction of generated voltage due to the narrow active piezoelectric regions between the IDE fingers, the increment of output current is vital for operating the flexible electronics because the output voltage is already sufficient for f-VLED operation. Interestingly at below 50 μm spacing, the energy harvester suffered electrical damage during a later poling process. To prevent electrical breakdown caused by mechanical cracks in the PZT thin film, an SU-8 epoxy layer was coated on the IDE-patterned PZT energy harvester. The final step for the flexible energy harvester is a poling process performed by electrical fields of 100 kV cm^{-1} at 120 °C. This poling process is basically derived from the principle that most of the dipoles are aligned parallel to the direction of the applied electrical field and permanently maintain their polarity, even after removing the electrical field. Finally, the AlGaInP f-VLEDs interconnected with the PZT thin-film energy harvester defined as 'self-powered fully-flexible light-emitting system' was fabricated, as illustrated in Fig. 1c. The self-powered f-VLEDs can be driven by the electricity generated from the slight bending deformations of the flexible piezoelectric energy harvester. The details of the fabrication methods are described in the experimental section and ESI.†

Characterisation of f-VLEDs

Fig. 2a shows the optical photograph of the 4 × 4 f-VLEDs array of crossbar structures (top inset). The ACF electrically connects the f-VLED chips to the bottom electrodes with no electrical breakdown or leakage. Fig. 2b is the luminance–current–voltage (*L–I–V*) and optical power characteristic curves of a representative f-VLED device after the ACF bonding process with various

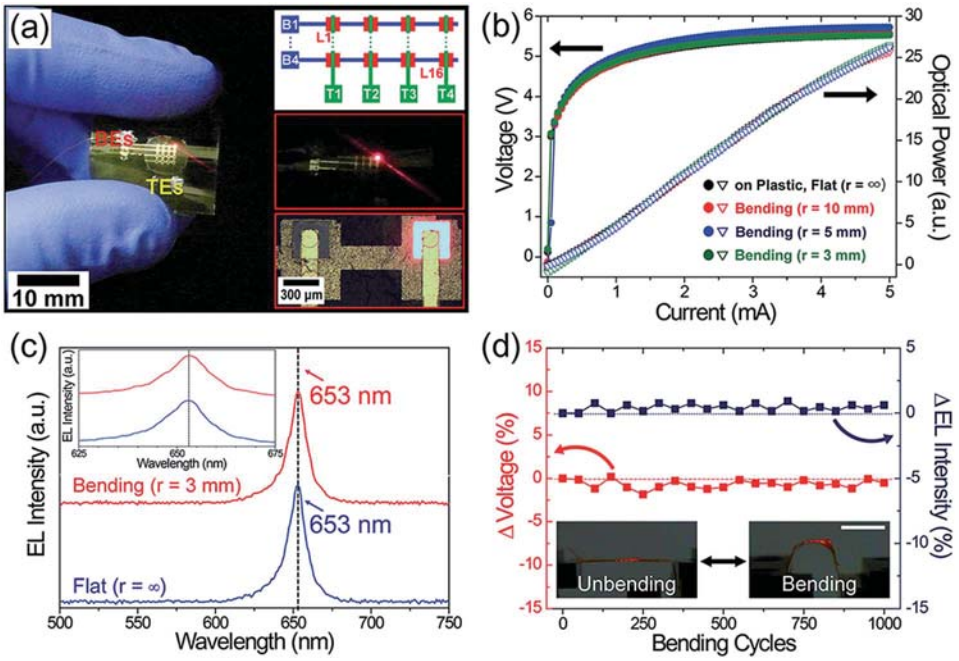

Fig. 2 (a) A representative photograph showing a crossbar-structured f-VLEDs array with one turned-on VLED. (Top inset) the scheme of the crossbar structure of the VLEDs array; (middle inset) the turned-on f-VLED in a dark room; and (bottom inset) an optical microscopy image of the turned-on f-VLED. (b) Luminance–current–voltage (*L–I–V*) measurements of VLEDs on a flat plastic substrate, and a bent plastic substrate with bending radii of 10 mm, 5 mm, and 3 mm. (c) Spectra of the emission from the f-VLEDs at flat and bending states. The inset shows the magnified spectral properties in the emission wavelength region (near 653 nm). (d) Mechanical durability test of f-VLEDs to investigate the stability of f-VLEDs. The inset shows a bending radius (10 mm); scale bar, 1 cm.

bending radii. These characteristics did not substantially change after bending deformation on a plastic substrate with varied radii of curvature down to 3 mm. The turn-on voltage of the f-VLED was measured to be about 3 V, which was sufficiently low to be driven by voltage from our flexible energy harvester. In addition, the electroluminescence (EL) spectral property (peak wavelength ≈ 653 nm) of the f-VLED in the bent state was almost identical to the f-VLED device under flat condition (Fig. 2c). In contrast with previous reports on flexible lateral inorganic LEDs,[46] our f-VLED did not show serious wavelength shift behaviours in the EL spectrum under bending conditions without the elimination of strain effects (mechanical neutral plane treatment), presumably because the short vertical current path of the f-VLED can be rarely affected by the mechanical bending stress compared to the long detour current path of the flexible lateral LED.[39,50] The mechanical stability of the flexible LEDs is of great importance for the future biomedical and commercial applications of flexible optoelectronic units. The durability of f-VLED was evaluated through over-extended bending cycles (~1000 cycles) with a bending radius of 5 mm, as shown in Fig. 2d. The EL intensity and the forward voltage (V_f) of the f-VLED at 5 mA were reliable without any significant change during the mechanical durability test. These results confirm that our f-VLED device is highly stable after the ACF bonding processes and periodic bending/unbending cycles, which are directly related to its mechanical robustness and its compatibility with a flexible piezoelectric energy-harvesting device.

To operate the f-VLEDs array using our self-powered flexible energy harvester, we designed f-VLED devices interconnected in series. The nine serial-connected f-VLEDs were successfully turned on in both flat and bending states under the input current of 1 mA (Fig. 3a). To estimate the electrical compatibility of f-VLEDs with our flexible piezoelectric thin-film energy harvester, we investigated the operating conditions of the serial f-VLEDs, such as electrical pulse width and current level. Because the voltage output of the flexible PZT thin-film energy harvester (≫100 V) is sufficient enough for driving the serial f-VLEDs, the determinant for the self-powered optoelectronic systems is the current level generated from the flexible energy harvester. As shown in Fig. 3b, the f-VLEDs array was well operated by an input current of 5 μA, corresponding with the output current generated from our flexible thin-film energy harvester. The turn-on voltage of the f-VLEDs at the energy harvester-compatible current level in serial connection is about 22.5 V (that of one VLED is approximately 2.5 V). The input signal shape is another important factor because the electrical output signals are discrete AC pulses. As presented in the inset of Fig. 3b and ESI Video S1,† the serial-connected f-VLEDs can be driven by the periodic 5 μA current pulses with full width at half-maximum (FWHM) of ~50 ms, corresponding to typical energy harvester signals (Fig. S5 in ESI†). Note that the deviated tails of measured voltage curve (see the black arrow in the inset of Fig. 3b) between the input current pulses (at a zero current region) were caused by the diffusion capacitance of the LED p–n diode during the turn-off transient.[51,52] As shown in Fig. S6,† the periodic voltage input with an FWHM of ~50 ms can also successfully operate the f-VLEDs.

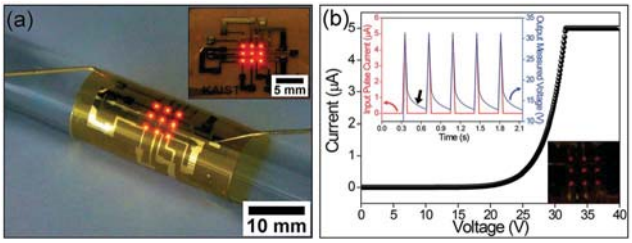

Fig. 3 (a) Photographs of a 3 × 3 array of f-VLEDs in a bent state on a glass rod (radius of curvature = 5 mm) and in a flat state (inset). All VLED chips are connected in series. The driving current of the source-meter is 1 mA for both cases. (b) An *I*–*V* curve of the serial-connected f-VLEDs array with current compliance of 5 μA, which shows that the generated current level from a flexible thin film energy harvester is able to operate the f-VLEDs. The bottom inset presents the optical image of turned-on f-VLEDs with driving current of 5 μA. The top inset demonstrates that pulsed input current signals (FWHM of 50 ms corresponding to generated signals of energy harvester) can operate the f-VLEDs. The tails of measured output voltage (non-zero voltage) between the input current pulses (at a zero current region) is due to the diffusion capacitance (charge storage capacitance) of the diode device during the turn-off transient.

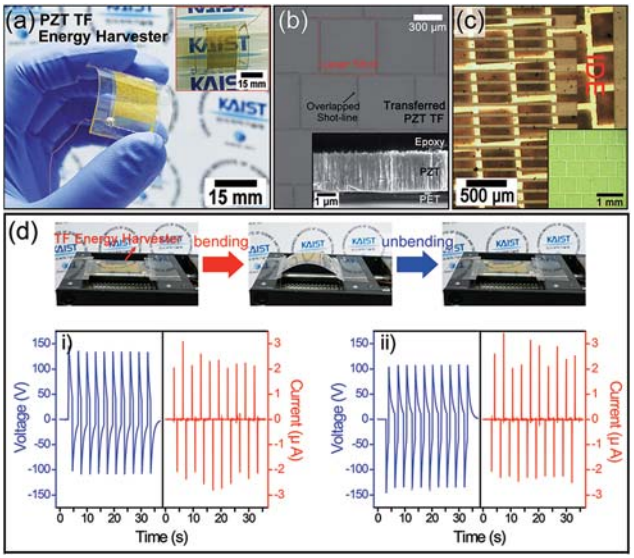

Fig. 4 (a) The flexible PZT thin-film (TF) energy harvester bent by fingers and attached to a glass tube (inset). (b) An SEM image of PZT thin film transferred to a PET substrate by 2D laser, which leaves square shot-patterns. The inset shows a cross-sectional SEM image of the PZT thin film after the LLO process. (c) The local optical micrograph of IDE on the PZT thin film with an epoxy passivation layer. No mechanical or electrical damage is observed during poling process and bending test. The inset is an optical microscopy image of PZT thin film before the formation of IDEs. (d) During bending and unbending motions of the energy-harvester device by a linear motor, the generated open-circuit voltage and short-circuit current from the flexible PZT thin-film energy harvester in (i) forward and (ii) reverse connections with a measurement instrument.

Output performance of thin-film energy harvester

A flexible PZT thin-film energy harvester (size of 2 cm × 5 cm) for operating the inorganic f-VLEDs appears in Fig. 4a. The energy harvester maintains outstanding piezoelectric properties as well as mechanical flexibility after the LLO process. Fig. 4b shows the scanning electron microscopy (SEM) images of 2 μm thick PZT layer transferred onto a plastic substrate by the irradiation of two-dimensional (2D) XeCl laser beam (625 μm × 625 μm). When the laser with the optimised energy density (420 mJ cm^{-2}) was irradiated, there were square shot-traces with overlapped regions of laser beams, as presented in Fig. 4b. During the LLO process of transferring the PZT thin film onto the flexible substrate neither mechanical damage (*e.g.*, cracks or wrinkles) nor the degradation of piezoelectric properties in the PZT layer was caused. As shown in the inset of Fig. 4b and S10,† neither crack nor mechanical failure was observed through the entire thickness of the PZT thin film during the LLO process. The maintenance of crystallinity, tetragonal phase (non-centrosymmetric perovskite crystal), and piezoelectric response of the transferred PZT thin film after the LLO process is also confirmed by X-ray diffraction (XRD), Raman spectroscopy, and piezoresponse force microscopy (PFM) analyses, respectively, as presented in Fig. S7.† The representative microscopic morphology of the PZT surface after transfer by the optimum laser intensity (the high-resolution SEM image in Fig. S9a†) includes a uniform nanoscale-bubbled structure created by laser-induced local melting and dissociation. However, the overpowered laser possibly induces macroscopic mechanical failures and morphological irregularities, such as agglomerated-topology on the transferred PZT surface (Fig. S8 and S9b in ESI†) because the excessively molten and decomposed PZT parts cannot uniformly solidify on the surface during the very short pulse duration (~30 ns) of XeCl excimer laser. The non-uniform agglomerates might be the potential origins of mechanical cracks and surface instabilities because rapid quenching by short-pulse duration can prevent the unevenly distributed stress to get energetically relaxed.[53] Fig. 4c is an optical microscopy image of the IDE-type energy harvester, which can generate higher output power from bending motions, compared to the MIM-type energy harvester.[5] The generated voltage and current corresponding to the mechanical deformation of the flexible energy harvester, is presented in Fig. 4d: bending and unbending states. The flexible PZT thin-film energy harvester produced the open-circuit voltage of ~140 V and the short-circuit current of ~3 μA by bending/unbending at a programmed bending machine (strain of ~0.205% at strain rate of ~2.32% s^{-1}). Although the strain in the PZT layer before passivation was about 0.39% which is higher than fracture strain of PZT,[54–56] the effective reduced strain in the PZT thin film with the SU-8 passivation layer was about 0.205%, when the bending radius was 1.61 cm (see the calculations in ESI†). To confirm that the measured output signals were generated by a true piezoelectric effect, a switching polarity test was performed

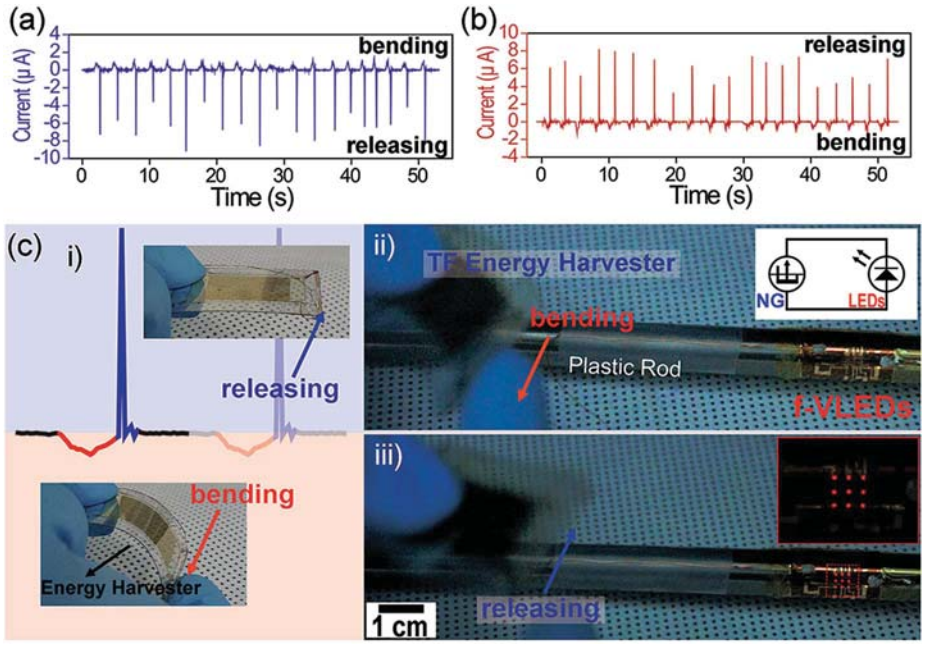

Fig. 5 (a and b) Current signals generated from the flexible PZT thin-film (TF) energy harvester by human finger flicking in (a) forward and (b) reverse connections using a measurement instrument. (c) Operation of a final self-powered flexible light-emitting system. (i) Photographs of PZT thin-film energy harvester at bent and released states, and corresponding produced current signals. (ii) The flexible energy harvester directly connected to the f-VLEDs array wrapping a plastic rod (radius of curvature = 5 mm) is bent by human fingers. (iii) When the flexible PZT thin-film energy harvester is released, the generated electrical energy is sufficient to drive the f-VLEDs array without any external energy sources or circuits. The light-emitting region (red dotted line) is magnified in the inset. In the captured photographs, the energy-harvester part is somewhat out-of-focus to show the operating f-VLEDs. In ESI Video S1,† various angles of the operating self-powered flexible light-emitting system can be seen.

to compare forward and reverse connections with measurement equipment (Fig. 4d-i and ii). The electromechanical energy-conversion efficiency was estimated as 11.8%, as calculated in ESI.† To directly harvest biomechanical energy, the thin-film energy harvester was also conformally attached on a human wrist (Fig. S16†). By the movement of the wrist, the electricity can be produced from the energy harvester up to a voltage of 120 V and a current of 2 μA.

Operation of self-powered all-flexible light-emitting system

To clarify that the self-powered flexible electronics can be readily fulfilled in everyday life, we utilised mechanical energy from human finger motions to spontaneously drive the f-VLEDs. Fig. 5 (a and b) shows the self-sufficient current (5–10 μA) generated by periodically flicking the flexible thin-film energy harvester using human fingers. Note that biomechanical stimuli can produce higher current levels, compared to the regulated movements of bending machines due to the fast strain rate. As presented in the magnified current peaks by finger bending and releasing (Fig. 5c-i), the releasing motions of the flexible energy harvester generated high and sharp current signals, while the bending motions of the flexible energy harvester produced low and broad current peaks owing to the uncertainty of strain rates by finger flicking. Therefore, the resulting current signal from the releasing deformation was considered to be suitable to drive the f-VLEDs, as proven in Fig. 3 and S5.† Using this output current and on the basis of our previous investigations, we were successful in turning on the f-VLEDs array using the self-sufficient energy. The f-VLEDs on a curvilinear plastic rod were directly operated by finger-induced deformation of the flexible energy harvester without any rectifiers or storage devices. The equivalent electrical circuit diagram for this self-powered electronic system is shown in the inset of Fig. 5c-ii. At the releasing moment of the flexible energy harvester, the f-VLEDs array was simultaneously turned on, as displayed in the captured image of Fig. 5c-iii and the inset (see ESI Video S1† for a movie clip showing the self-powered flexible light-emitting system operated by the deformation of the thin-film energy harvester). These results fully demonstrate that our high-performance, flexible thin-film energy harvester can serve as reliable energy for self-sufficient flexible optoelectronic devices. AC–DC converting technologies combined with power management circuits require further investigations for self-powered flexible systems to be used in universal electronics.

Conclusions

To conclude, we have successfully demonstrated an unprecedented concept of self-powered fully-flexible electronics using a highly-efficient piezoelectric energy harvester on a very thin flexible plastic substrate, which are compatibly driven by fingering motions. Using the flexible PZT thin-film energy harvester, we have successfully operated a flexible vertically structured, light-emitting diode (f-VLEDs) array on a curvilinear surface. Moreover, the red emitting f-VLEDs, fabricated by the ACF bonding process and the wet etching of an entire GaAs mother wafer, have been driven with remarkable performance stability (*e.g.*, *L–I–V* characteristics and turn-on voltage) by a relatively small and irregular self-powered flexible energy source from repeated bending. The characteristics of the f-VLED were maintained in the deformed state (with a bending radius as small as 3 mm) on a curvilinear surface. During repeated bending/releasing motions, the flexible PZT thin-film energy harvester fabricated by an LLO process produced both high-output voltage and current (~140 V and ~10 μA) through slight finger motions, and could directly operate the 3 × 3 f-VLEDs array without any external energy supplies or circuits. Our facile fusion technology for self-powered flexible electronic systems can be applied to various practical devices, such as bio-implantable applications (*e.g.*, optical biosensors, photo-therapy, and optogenetics) and microelectromechanical systems (MEMS)[57,58] as well as mobile/wearable optoelectronics. We are currently investigating the self-powered flexible system on single flexible substrate to achieve a miniaturised and self-containing system. We are also making efforts for the power enhancement of flexible energy sources using multi-layer stacking or single-crystalline piezoelectric materials to accomplish the advanced requirements of practical electronic applications.

Experimental

Fabrication steps for the f-VLEDs of the self-powered flexible light-emitting system

A designed GaAs epitaxial wafer (Kodenshi Co., wavelength range of 640–660 nm) was dry-etched with patterned photoresist (PR) for the size of microscale LED chips. The detailed structure of the GaAs epitaxial wafer is shown in Fig. S2.† The dry etching was performed by inductively coupled plasma reactive ion etching (ICP-RIE) with the gas environment of Cl_2/Ar (40 sccm/5 sccm). After the O_2 plasma treatment for PR removal, Ti/Au (10 nm/100 nm) thin films were deposited and patterned on the LED chips by radio frequency sputtering and photolithography. On a PI substrate (25 μm in thickness, Kapton film, DuPont), Cr/Au metal layers for bottom electrodes were also deposited and patterned by the same methods. An ACF film (H&S HighTech) was sandwiched between the GaAs wafer with the LED chips and the bottom electrode-patterned PI substrate. To perform the main ACF bonding process for the formation of vertically anisotropic current paths, pressure (1 MPa) was applied to the sandwiched specimen at 245 °C for 75 s. During the ACF bonding process, the LED chips were flipped over; the p-type GaP window layers became the bottom region of the f-VLED chips and the GaInP etch-stop and n-type confinement layers became the top region of the f-VLED chips. To protect the device regions during the wet etching for the removal of GaAs mother wafer, the ACF-bonded specimen was encapsulated by PR (AZ 5214, MicroChem) and plastic paraffin film, except for the backside of the GaAs wafer. The GaAs wafer was removed by wet-etching at 45 °C using wet etchant composed of NH_4OH and H_2O_2 (volume ratio of 1 : 6). After the complete removal of the GaAs mother wafer, the f-VLEDs were passivated by an SU-8 epoxy layer (MicroChem, 10 μm in thickness) except for the top

regions of the VLED chips. Finally, Ti/Au thin films were deposited and patterned to form the top electrodes connected with the top region of the f-VLEDs. The schematic illustrations of fabrication steps for the f-VLEDs are shown in Fig. S1 in ESI.†

Fabrication steps for the PZT thin-film energy harvester of the self-powered flexible light-emitting system

The PZT thin film was deposited by a conventional sol–gel process on a double-sided polished sapphire wafer (430 μm in thickness, Hi-Solar Co.). The PZT sol–gel solution of 0.4 M (52 : 48 molar ratio of Zr : Ti with 10 mol% excess PbO, MEMS Solution Co.) was spin-casted on the wafer at 2500 rpm followed by pyrolysis in air environment at 450 °C for 10 min, to remove organic components from the sol–gel solution thin film. These deposition and pyrolysis steps were repeated several times to form a PZT thin film of 2 μm in thickness. Crystallisation of the PZT thin film was performed in air at 650 °C for 45 min. Rapid thermal annealing (RTA) was used for the pyrolysis and crystallisation processes. The PZT thin film on the sapphire substrate was conformally attached to a PET substrate (125 μm in thickness, Sigma-Aldrich) by a UV-sensitive PU adhesive (Norland Optical Adhesive No. 73, Norland Products Inc.), which was completely cured by a UV light source with a power density of 6 mW cm^{-2} for 30 min. After exposure to UV light for curing the PU adhesive, a 2D pulsed XeCl excimer laser (wavelength of 308 nm, area of 625 μm × 625 μm) was used to irradiate the backside of the sapphire substrate to separate the PZT thin film from the sapphire substrate. The optimised energy density of the laser beam was found to be 420 mJ cm^{-2}. After this LLO process to transfer the PZT thin film to the flexible PET substrate, IDEs with an electrode width of 100 μm and an inter-electrode gap of 50 μm were defined on the PZT thin film by Cr- and Au-sputtering (110 nm in thickness) and standard photolithography processes. To protect this energy-harvester device from mechanical and electrical damage, the entire PZT thin film and IDEs were encapsulated by SU-8 epoxy (MicroChem, 5 μm in thickness) using direct spin-coating and curing at 105 °C for 4 min, except the metal contact holes for wiring. Finally, a poling process to align dipoles in the PZT thin film was conducted using electrical fields of 100 kV cm^{-1} at 120 °C for 3 h.

Acknowledgements

This work was supported by the Basic Science Research Program (grant code: NRF-2012R1A2A1A03010415) and Center for Integrated Smart Sensors as Global Frontier Project (CISS-2012M3A6A6054187) funded by the Korean government (MSIP) through the National Research Foundation of Korea (NRF).

Notes and references

1 K.-I. Park, S. Xu, Y. Liu, G.-T. Hwang, S.-J. L. Kang, Z. L. Wang and K. J. Lee, *Nano Lett.*, 2010, **10**, 4939–4943.
2 K.-I. Park, M. Lee, Y. Liu, S. Moon, G.-T. Hwang, G. Zhu, J. E. Kim, S. O. Kim, D. K. Kim, Z. L. Wang and K. J. Lee, *Adv. Mater.*, 2012, **24**, 2999–3004.
3 K.-I. Park, C. K. Jeong, J. Ryu, G.-T. Hwang and K. J. Lee, *Adv. Energy Mater.*, 2013, **3**, 1539–1544.
4 C. K. Jeong, I. Kim, K.-I. Park, M. H. Oh, H. Paik, G.-T. Hwang, K. No, Y. S. Nam and K. J. Lee, *ACS Nano*, 2013, **7**, 11016–11025.
5 K.-I. Park, J. H. Son, G.-T. Hwang, C. K. Jeong, J. Ryu, M. Koo, I. Choi, S. H. Lee, M. Byun, Z. L. Wang and K. J. Lee, *Adv. Mater.*, 2014, **26**, 2514–2520.
6 C. K. Jeong, K.-I. Park, J. Ryu, G. T. Hwang and K. J. Lee, *Adv. Funct. Mater.*, 2014, **24**, 2620–2629.
7 G.-T. Hwang, H. Park, J. H. Lee, S. Oh, K. I. Park, M. Byun, G. Ahn, C. K. Jeong, K. No, H. Kwon, S. G. Lee, B. Joung and K. J. Lee, *Adv. Mater.*, 2014, **26**, 4880–4887.
8 S. Y. Lee, K.-I. Park, C. Huh, M. Koo, H. G. Yoo, S. Kim, C. S. Ah, G. Y. Sung and K. J. Lee, *Nano Energy*, 2012, **1**, 145–151.
9 S. Kim, H. Y. Jeong, S. K. Kim, S. Y. Choi and K. J. Lee, *Nano Lett.*, 2011, **11**, 5438–5442.
10 M. Koo, K.-I. Park, S. H. Lee, M. Suh, D. Y. Jeon, J. W. Choi, K. Kang and K. J. Lee, *Nano Lett.*, 2012, **12**, 4810–4816.
11 G.-T. Hwang, D. Im, S. E. Lee, J. Lee, M. Koo, S. Y. Park, S. Kim, K. Yang, S. J. Kim, K. Lee and K. J. Lee, *ACS Nano*, 2013, **7**, 4545–4553.
12 H. G. Yoo, S. Kim and K. J. Lee, *RSC Adv.*, 2014, **4**, 20017–20023.
13 M. Koo, S. Y. Park and K. J. Lee, *Nanobiosensors in Disease Diagnosis*, 2012, **1**, 5–15.
14 S. H. Lee, S. Y. Park and K. J. Lee, *Proc. SPIE*, 2012, **8460**, 846011.
15 Z. L. Wang and W. Wu, *Angew. Chem., Int. Ed.*, 2012, **51**, 11700–11721.
16 C. Dagdeviren, B. D. Yang, Y. Su, P. L. Tran, P. Joe, E. Anderson, J. Xia, V. Doraiswamy, B. Dehdashti, X. Feng, B. Lu, R. Poston, Z. Khalpey, R. Ghaffari, Y. Huang, M. J. Slepian and J. A. Rogers, *Proc. Natl. Acad. Sci. U. S. A.*, 2014, **111**, 1927–1932.
17 J. Viventi, D.-H. Kim, L. Vigeland, E. S. Frechette, J. A. Blanco, Y.-S. Kim, A. E. Avrin, V. R. Tiruvadi, S.-W. Hwang, A. C. Vanleer, D. F. Wulsin, K. Davis, C. E. Gelber, L. Palmer, J. Van der Spiegel, J. Wu, J. Xiao, Y. Huang, D. Contreras, J. A. Rogers and B. Litt, *Nat. Neurosci.*, 2011, **14**, 1599–1605.
18 D.-H. Kim, J. Viventi, J. J. Amsden, J. Xiao, L. Vigeland, Y.-S. Kim, J. A. Blanco, B. Panilaitis, E. S. Frechette, D. Contreras, D. L. Kaplan, F. G. Omenetto, Y. Huang, K.-C. Hwang, M. R. Zakin, B. Litt and J. A. Rogers, *Nat. Mater.*, 2010, **9**, 511–517.
19 A. Chirilă, S. Buecheler, F. Pianezzi, P. Bloesch, C. Gretener, A. R. Uhl, C. Fella, L. Kranz, J. Perrenoud, S. Seyrling, R. Verma, S. Nishiwaki, Y. E. Romanyuk, G. Bilger and A. N. Tiwari, *Nat. Mater.*, 2011, **10**, 857–861.
20 G. Li, R. Zhu and Y. Yang, *Nat. Photonics*, 2012, **6**, 153–161.
21 G. A. T. Sevilla, S. Bin Inayat, J. P. Rojas, A. M. Hussain and M. M. Hussain, *Small*, 2013, **9**, 3916–3921.
22 T. Park, C. Park, B. Kim, H. Shin and E. Kim, *Energy Environ. Sci.*, 2013, **6**, 788–792.

23 S. J. Kim, J. H. We and B. J. Cho, *Energy Environ. Sci.*, 2014, **7**, 1959–1965.
24 Y. Hu, Y. Zhang, C. Xu, G. Zhu and Z. L. Wang, *Nano Lett.*, 2010, **10**, 5025–5031.
25 X. S. Zhang, M. D. Han, R. X. Wang, F. Y. Zhu, Z. H. Li, W. Wang and H. X. Zhang, *Nano Lett.*, 2013, **13**, 1168–1172.
26 G. Zhu, R. Yang, S. Wang and Z. L. Wang, *Nano Lett.*, 2010, **10**, 3151–3155.
27 Z. L. Wang, *Sci. Am.*, 2008, **298**, 82–87.
28 T. D. Nguyen, N. Deshmukh, J. M. Nagarah, T. Kramer, P. K. Purohit, M. J. Berry and M. C. McAlpine, *Nat. Nanotechnol.*, 2012, **7**, 587–593.
29 S. Lee, S. H. Bae, L. Lin, Y. Yang, C. Park, S. W. Kim, S. N. Cha, H. Kim, Y. J. Park and Z. L. Wang, *Adv. Funct. Mater.*, 2013, **23**, 2445–2449.
30 J. Yoon, S. Jo, I. S. Chun, I. Jung, H.-S. Kim, M. Meitl, E. Menard, X. Li, J. J. Coleman, U. Paik and J. A. Rogers, *Nature*, 2010, **465**, 329–333.
31 R.-H. Kim, D.-H. Kim, J. Xiao, B. H. Kim, S.-I. Park, B. Panilaitis, R. Ghaffari, J. Yao, M. Li, Z. Liu, V. Malyarchuk, D. G. Kim, A.-P. Le, R. G. Nuzzo, D. L. Kaplan, F. G. Omenetto, Y. Huang, Z. Kang and J. A. Rogers, *Nat. Mater.*, 2010, **9**, 929–937.
32 S.-I. Park, Y. Xiong, R.-H. Kim, P. Elvikis, M. Meitl, D.-H. Kim, J. Wu, J. Yoon, C.-J. Yu, Z. Liu, Y. Huang, K. Hwang, P. Ferreira, X. Li, K. Choquette and J. A. Rogers, *Science*, 2009, **325**, 977–981.
33 R.-H. Kim, H. Tao, T.-I. Kim, Y. Zhang, S. Kim, B. Panilaitis, M. Yang, D.-H. Kim, Y. H. Jung, B. H. Kim, Y. Li, Y. Huang, F. G. Omenetto and J. A. Rogers, *Small*, 2012, **8**, 2812–2818.
34 T. Kim, J. G. McCall, Y. H. Jung, X. Huang, E. R. Siuda, Y. Li, J. Song, Y. M. Song, H. A. Pao, R.-H. Kim, C. Lu, S. D. Lee, I.-S. Song, G. Shin, R. Al-Hasani, S. Kim, M. P. Tan, Y. Huang, F. G. Omenetto, J. A. Rogers and M. R. Bruchas, *Science*, 2013, **340**, 211–216.
35 J. G. McCall, T. Kim, G. Shin, X. Huang, Y. H. Jung, R. Al-Hasani, F. G. Omenetto, M. R. Bruchas and J. A. Rogers, *Nat. Protoc.*, 2013, **8**, 2413–2428.
36 B. H. Morris, J. E. Tyson, D. K. Stevenson, W. Oh, D. L. Phelps, T. M. O'Shea, G. E. McDavid, K. P. Van Meurs, B. R. Vohr, C. Grisby, Q. Yao, S. Kandefer, D. Wallace and R. D. Higgins, *J. Perinatol.*, 2013, **33**, 126–133.
37 A. P. C. Sousa, G. M. Paraguassú, N. T. T. Silveira, J. Souza, M. C. T. Cangussú, J. N. Santos and A. L. B. Pinheiro, *Lasers Med. Sci.*, 2013, **28**, 981–987.
38 C. A. Tran, C. F. Chu, C. C. Cheng, W. H. Liu, J. Y. Chu, H. C. Cheng, F. H. Fan, J. K. Yen and T. Doan, *J. Cryst. Growth*, 2007, **298**, 722–724.
39 C.-F. Chu, C.-C. Cheng, W.-H. Liu, J.-Y. Chu, F.-H. Fan, H.-C. Cheng, T. Doan and C. A. Tran, *Proc. IEEE*, 2010, **98**, 1197–1207.
40 R.-H. Kim, S. Kim, Y. M. Song, H. Jeong, T.-I. Kim, J. Lee, X. Li, K. D. Choquette and J. A. Rogers, *Small*, 2012, **8**, 3123–3128.
41 N. C. Klapoetke, Y. Murata, S. S. Kim, S. R. Pulver, A. Birdsey-Benson, Y. K. Cho, T. K. Morimoto, A. S. Chuong, E. J. Carpenter, Z. Tian, J. Wang, Y. Xie, Z. Yan, Y. Zhang, B. Y. Chow, B. Surek, M. Melkonian, V. Jayaraman, M. Constantine-Paton, G. K.-S. Wong and E. S. Boyden, *Nat. Methods*, 2014, **11**, 338–346.
42 H. T. Whelan, R. L. Smits, E. V Buchman, N. T. Whelan, S. G. Turner, D. A. Margolis, V. Cevenini, H. Stinson, R. Ignatius, T. Martin, J. Cwiklinski, A. F. Philippi, W. R. Graf, B. Hodgson, L. Gould, M. Kane, G. Chen and J. Caviness, *J. Clin. Laser Med. Surg.*, 2001, **19**, 305–314.
43 M. Ishiguro, K. Ikeda and K. Tomita, *J. Orthop. Sci.*, 2010, **15**, 233–239.
44 M.-J. Yim and K.-W. Paik, *IEEE Trans. Compon., Packag., Manuf. Technol., Part A*, 1998, **21**, 226–234.
45 W. S. Kwon and K. W. Paik, *Int. J. Adhes. Adhes.*, 2004, **24**, 135–142.
46 S.-I. Park, A.-P. Le, J. Wu, Y. Huang, X. Li and J. A. Rogers, *Adv. Mater.*, 2010, **22**, 3062–3066.
47 D. Simeonov, E. Feltin, A. Altoukhov, A. Castiglia, J.-F. Carlin, R. Butté and N. Grandjean, *Appl. Phys. Lett.*, 2008, **92**, 171102.
48 K. R. Williams and R. S. Muller, *J. Microelectromech. Syst.*, 1996, **5**, 256–269.
49 Y. H. Do, M. G. Kang, J. S. Kim, C. Y. Kang and S. J. Yoon, *Sens. Actuators, A*, 2012, **184**, 124–127.
50 C.-K. Li and Y.-R. Wu, *IEEE Trans. Electron Devices*, 2012, **59**, 400–407.
51 M. L. Lucia, J. L. Hernandez-Rojas, C. Leon and I. Mártil, *Eur. J. Phys.*, 1993, **14**, 86–89.
52 C.-L. Liao, Y.-F. Chang, C.-L. Ho and M.-C. Wu, *IEEE Electron Device Lett.*, 2013, **34**, 611–613.
53 J. Gayda, P. Kantzos and J. Miller, *Pract. Fail. Anal.*, 2003, **3**, 55–59.
54 O. Guillon, F. Thiebaud and D. Perreux, *Int. J. Fract.*, 2002, **117**, 235–246.
55 Y. Qi, J. Kim, T. D. Nguyen, B. Lisko, P. K. Purohit and M. C. McAlpine, *Nano Lett.*, 2011, **11**, 1331–1336.
56 X. Feng, B. D. Yang, Y. Liu, Y. Wang, C. Dagdeviren, Z. Liu, A. Carlson, J. Li, Y. Huang and J. A. Rogers, *ACS Nano*, 2011, **5**, 3326–3332.
57 A. Koka and H. A. Sodano, *Nat. Commun.*, 2013, **4**, 2682.
58 A. Koka, Z. Zhou and H. A. Sodano, *Energy Environ. Sci.*, 2014, **7**, 288–296.